J|A|C|S
ARTICLES
Published on Web 02/01/2003

Structural and Vibrational Study of the Tautomerism of Histamine Free-Base in Solution

F. Javier Ramírez,*,† Iñaki Tuñón,‡ Juan A. Collado,† and Estanislao Silla‡

Contribution from the Departamento de Química Física, Facultad de Ciencias, Universidad de Málaga, Campus de Teatinos, 29071-Málaga, Spain, and Departamento de Química Física/IcMol, Facultad de Químicas, Universidad de Valencia, 46100-Burjassot (Valencia), Spain

Received May 30, 2002; E-mail: ramirez@uma.es

Abstract: Infrared and Raman spectroscopy in H_2O and D_2O and quantum Density Functional calculations were used to determine the structure of histamine free-base in aqueous solution. A quantum mechanical study of the tautomeric equilibrium of histamine free-base in solution was performed at the 6-311G** level. Electronic correlation energies were included by using the hybrid functional B3LYP. The solvent was simulated as a continuum characterized by a dielectric constant, and the quantum system (solute) was placed in an ellipsoidal cavity. Solute−solvent electrostatic interaction was calculated by means a multipolar moment expansion introduced in the Hamiltonian. Four relevant histamine conformations were optimized by allowing all the geometrical parameters to vary independently, which involved both the gauche−trans and the N3H−N1H tautomerisms. The calculated free energies predicted N3H-gauche as the most stable one of histamine free-base in solution. The order of stability is here completely altered with respect to previous results in gas phase, which presented the N1H-gauche conformer as the most stable structure. Our results also differ from previous Monte Carlo simulations, which obtained the N3H-trans conformer as the most stable in solution, although in this case, the histamine structures were kept frozen to the gas-phase geometry. Vibrational spectroscopy results support theoretical ones. Quadratic force fields for the four histamine conformers were achieved under the same calculation methodology. Previously, a general assignment of the infrared and Raman spectra of histamine free-base was proposed for solutions in both natural and heavy water. This allowed us to compare the experimental set of both wavenumbers and infrared intensities with the calculated ones. The lowest quadratic mean wavenumber deviation was obtained for the N3H-gauche conformer, in agreement with the free-energy calculations. Calculated infrared intensities were also compared to the experimental intensities, supporting this conformer as the relevant structure of histamine free-base in solution. It was then selected for a complete vibrational dynamics calculation, starting with a low-level scaling procedure to fit the set of calculated wavenumbers to the experimental values. The results were presented in terms of quadratic force constants, potential energy distribution, and normal modes.

Introduction

Biogenic amine histamine (2-aminoethyl imidazole) is a simple molecule involved in several defense mechanisms of the body.[1] It is widely distributed in both vegetal and animal kingdoms, from unicellular to superior organisms.[2] The biological activity of histamine is related with specific receptors on the cell membranes,[1,3] having different responses depending on the receptor. The interaction with H1 receptors stimulates muscle contraction, vasodilatation, drop in blood pressure, etc. The interaction with H2 receptors stimulates stomach secretions, heart rhythm regulation, immunological reactions, etc.[4,5] Receptors H3 are involved in nervous transmission.[6] The relationships between histamine and allergies have been clearly established, as histamine is released when the body is invaded by external agents.[1] These important functions have aimed investigators toward the synthesis of related molecules that reproduce some of the histamine biological activity; thus, chlorpheniramine (gamma-(4-chlorphenyl),*N*,*N*-dimethyl-2-pyridinpropanoamine) has demonstrated to efficiently act in some allergic processes.[7] Interaction of these biogenic and synthetic amines with DNA, leading to conformational transitions, condensations, and other structural changes, has been proposed to explain some of their biological roles.[8−12]

† Universidad de Málaga.
‡ Universidad de Valencia.

(1) Green, J. P. *Handb. Neurochem.* **1970**, *4*, 221.
(2) Reite, O. B. *Physiol. Rev.* **1972**, *52*, 778.
(3) Hess, H. J. *Annu. Rep. Med. Chem.* **1968**, 56.
(4) Cooper, D. G.; Young, R. C.; Durant, G. J.; Ganellin, C. R. In *Comprenhensive Medicinal Chemistry*; Jammes, P. G., Taylor, J. B., Eds.; Pergamon Press: Oxford, 1990; Vol. 3.
(5) Voukydis, P. C. *Arch. Int. Pharmacodyn. Ther.* **1969**, *179*, 364.
(6) Monnier, M.; Saver, R. *Hatt AM Int. Rev. Neurobiol.* **1970**, *12*, 265.
(7) Medina, M. A.; Ramírez, F. J.; Ruiz-Chica, J.; Chavarría, T.; López-Navarrete, J. T.; Sánchez-Jiménez, F. *Biochim. Biophys. Acta* **1998**, *129*, 1379.
(8) Feuerstein, B. G.; Williams, L. D.; Basu, H. S.; Manton, L. J. *Proc. Natl. Acad. Sci. U.S.A.* **1986**, *83*, 5948.
(9) Schmid, N.; Behr, J. P. *Biochemistry* **1991**, *30*, 4357.

10.1021/ja027103x CCC: $25.00

The histamine molecule in aqueous solution is the result of a multiple acid−base equilibrium. The free-base, or neutral histamine, can accept one of two protons to give histamine monocation or dication, respectively. As a consequence, the pH of the medium and the two p*K*'s of histamine establish the concentration ratios among the three species. At pH values between 6.5 and 8.5 the predominant species, is the monocation (more than 80%), whereas at a pH lower than 5 that is the dication. At pH values greater than 10, the predominant species is the free-base. Only at an extremely basic pH, histamine rejects a proton giving the anion. On the other hand, both the monocation and the neutral form are able to exist in two tautomers, generated from the translation of the imidazole acidic hydrogen between the two nitrogen atoms. The biological significance of the histamine tautomerism has been demonstrated because it plays an important role in the mechanism of activation for H2 receptors.[13,14] The proposed mechanism, which has been theoretically supported from ab initio calculations,[15] involves the change in tautomeric preference when the positive charge of the side-chain is neutralized as a consequence of the interaction with the receptor.

In previous papers, we paid attention to the cationic species of histamine, which were studied from both the structural and the vibrational points of view. Vibrational spectra for solid[16,18] and solved[17,18] samples, including deuterated derivatives, in combination with quantum mechanical calculations[17] were performed. Solvent effects were simulated by means of a continuum model in which the solute is placed in an ellipsoidal cavity adapted to its form and size. Harmonic Cartesian force constants were evaluated using ab initio methodology at the 6-31+G* level. Electronic correlation was also included from the density functional theory (DFT),[19] which allows us for reliable correlation energies at computational costs significantly lower than the models based on the perturbation theory (Moller−Plesset, MP). In this paper, we have focused our attention on the neutral form.

No clear evidence has been previously achieved about the more stable conformers of neutral histamine in solution. As previously mentioned, two tautomeric forms can be expected for this molecule, usually named N^{π} (or N1−H) and N^{τ} (or N3−H), Figure 1, which differ on the relative position of the imidazole N−H bond respect to the side-chain. In addition, the structural flexibility of the side-chain allows it to adopt several conformations with respect to the imidazole ring. They have been classified into two main groups, named as trans (or extended) and gauche (or scorpio). Only one of these, the N^{π}-gauche tautomer, has the possibility of forming an intramolecular hydrogen bond between the imidazole N−H group and the N atom of the amino group. This fact makes it the most stable conformer of neutral histamine in gas phase, as theoretically

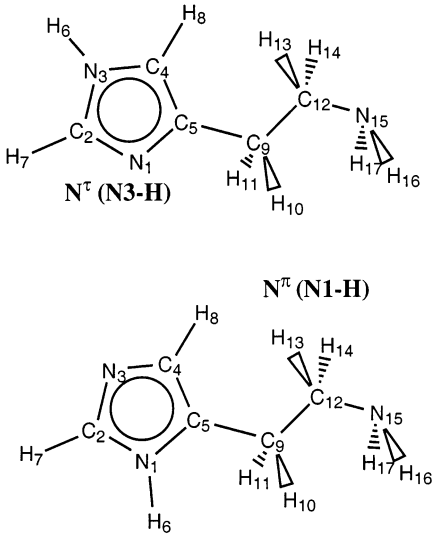

Figure 1. Two tautomeric forms of neutral histamine showing atom labeling.

demonstrated.[20−22] However, the rotational spectra of an isolated histamine molecule allowed detection of both N^{π} and N^{τ} species among the four more stable conformers.[20] We would like to emphasize that all of them were gauche and had very similar energies. This result was expected because of the absence of surrounding. In solid state, the strong intermolecular interactions usually froze a single structure. Thus, an X-ray diffraction study on crystals of histamine free-base[23] has demonstrated that the N^{π}-trans tautomer is the only species existing in solid state. The imidazole ring is a plane, and there are hydrogen bonds between the imidazole N−H group and the amino group of two adjacent molecules.

The only experimental work on the structure of neutral histamine in aqueous solution was reported in the 1970s from ^{13}C nuclear magnetic resonance spectroscopy.[24] The results indicated preference of the N^{τ} tautomer, which also was the predominant form of the monocation in solution.[25] However, the ratio of the N^{τ} to N^{π} tautomers appeared to be much greater for the monocation than for the free-base.[26] Theoretical calculations reported so far have given some contradictory results,[13,20−22,27−28] and the question about which is the most stable structure of neutral histamine in solution remains open. In the present work, we have performed quantum mechanical calculations, including electronic correlation energies and a continuum solvent model, on the structural properties and vibrational dynamics of different tautomeric forms of this molecule. Scaled quantum mechanical (SQM) force fields have been computed in order to compare the theoretical vibrational wavenumbers to those experimental. A general assignment of the fundamentals of neutral histamine in aqueous solution is

(10) *Biological and Therapeutic Implications of the Effects of Polyamines on Chromatin Condensatio*n; Casero, R. A., Jr., Ed.; R. G. Landes: Austin, TX, 1995.
(11) Thomas, T. J.; Thomas, T. *Biochem. J.* **1994**, *298*, 485.
(12) Thomas, T. J.; Ashley, C.; Thomas, T.; Shirahata, A.; Sigal, L. H.; Lee, J. S. *Biochem. Cell Biol.* **1997**, *75*, 207.
(13) Topiol, S.; Weisntein, H.; Osman, R. *J. Med. Chem.* **1984**, *27*, 1531.
(14) Worth, G. A.; King, P. M.; Richards, W. G. *Biochim. Biophys. Acta* **1990**, *158*, 1036.
(15) Weisntein, H.; Chou, E.; Johnson, C. L.; Kang, S.; Green, J. P. *Mol. Pharmacol.* **1976**, *12*, 738.
(16) Collado, J. A.; Ramírez, F. J. *J. Raman Spectrosc.* **1999**, *30*, 391.
(17) Collado, J. A.; Tuñón, I.; Silla, E.; Ramírez, F. *J. Phys. Chem. A* **2000**, *104*, 2120.
(18) Collado, J. A.; Ramírez, F. J. *J. Raman Spectrosc.* **2000**, *31*, 925.
(19) Parr, R. G.; Yang, W. *Density Functional Theory of Atoms and Molecules*; Oxford University Press: New York, 1989.
(20) Vogelsanger, B.; Godfrey, P. D.; Brown, R. D. *J. Am. Chem. Soc.* **1991**, *113*, 7864.
(21) Nagy, P. I.; Durant, G. J.; Hess, W. P.; Smith, D. A. *J. Am. Chem. Soc.* **1994**, *116*, 4898.
(22) Karpinska, G.; Dobrowolski, J. C.; Mazurek, A. P. *J. Mol. Struct. (THEOCHEM)* **1996**, *369*, 137.
(23) Bonnet, J. J.; Ibers, J. A. *J. Am. Chem. Soc.* **1975**, *95*, 4829.
(24) Wasylishen, R. E.; Tomlinson, G. *Can. J. Biochem.* **1977**, *55*, 579.
(25) Ganellin, C. R. *J. Pharm. Pharmacol.* **1973**, *25*, 787.
(26) Ganellin, C. R. In "*Pharmacology of Histamine Receptors*"; Ganellin, C. R., Parsons, M. E., Eds.; Wright PSG: Bristol, 1982; p 10.

proposed on the basis of the isotopic shifts upon deuteration and the reported assignments for the cationic species.[16−18] The paper has been organized as follows: first, we give the experimental and computational methodology, and second, the results are discussed in three sections, concerning (i) the structural properties (energies, geometrical parameters, charge distribution, etc.) of the selected tautomers, (ii) the experimental infrared and Raman spectra of histamine in solution of H_2O and D_2O, giving a general assigment of the observed bands, and (iii) a comparative vibrational study of the tautomers, in terms of vibrational wavenumbers and infrared intensities, taking into account the results obtained in the precedent section. Third, the lower energy conformer was selected to refine the ab initio force field to fit the calculated wavenumbers to those experimental. The results were presented in terms of normal modes, potential energy distribution and diagonal force constants.

Experimental Methods

Histamine free-base was purchased from Aldrich (99% purity), and was used without further treatment. Aqueous solutions at a concentration 1 M were prepared by using alternatively triply distilled water and deuterium oxide (99.9 atom % D, Aldrich). Taking into account the p*K* values of histamine free-base,[29] only 0.5% of the neutral molecules underwent to the monocation at the concentration used, giving rise to a final pH of about 11.5, as experimentally checked. This fact ensured therefore that the vibrational spectra of these solutions corresponded to neutral histamine.

Fourier transform infrared (FT-IR) and Raman (FT-Raman) spectra were recorded at the room temperature by means of a Bruker Equinox 55 spectrometer, purged with dry nitrogen. FT-IR spectra were obtained in a demountable cell for liquids and using a potassium bromide beam splitter. Suitable windows for aqueous solutions, made in calcium fluoride (1700−900 cm^{-1} region) and KRS-5 (1100−500 cm^{-1} region), were used. FT-Raman spectra were obtained using excitation radiation at 1064 nm from a Nd:YAG laser working at 500 mw; the samples were placed in a mirrored quartz cuvette and a calcium fluoride beam splitter was employed. A minimum of 500 scans was accumulated for all the spectra, at a resolution better than 2 cm^{-1}.

Theoretical Calculations

The solute−solvent electrostatic interaction was simulated employing the continuum model of Rivail et al.[30−32] In this model, the liquid was assimilated to a continuum characterized by a dielectric constant (78.4 for water). The quantum system was then placed in an ellipsoidal cavity whose volume was obtained by means of an empirical relation.[33] The electrostatic interaction was calculated using a multipolar moment expansion (up to sixth order) introduced in the Hamiltonian of the system. The analytical derivatives of this electrostatic term were evaluated leading to an efficient geometry optimization procedure.[34] Geometries were optimized using the redundant coordinate algorithm.[35] Cartesian force constants in solution were calculated at the fully optimized geometry using analytical second derivatives.[36] All of the calculations have been carried out using the hybrid functional B3LYP[37,38] and the 6-311G** basis set.[39,40] The GAUSSIAN98 package of programs[41] was employed. For consideration of continuum solvent effects an extra link[42] has been added. Nonelectrostatic contributions to the solvation free energy (dispersion/repulsion and cavitation) were calculated on the optimized structures according to the procedure of Tomasi et al. as implemented in GAUSSIAN98.[41] The relative value of these contributions was in any case less than 0.3 kcal/mol. Translational, rotational, and vibrational free energy contributions and zero-point energies were obtained using standard formulas.

Infrared absorption intensities were evaluated from the atomic polar tensors.[43] The Cartesian force constants were transformed into a set of nonredundant locally symmetrized internal coordinates, defined accordingly to the Pulay methodology.[44] This allows for a more useful description of the vibrational potential energy and makes further calculations easier. Quadratic force fields in internal coordinates were uniformly scaled with a single factor for all the conformers, which allowed for a direct wavenumber comparison. The force field for the most stable histamine conformer was further scaled with three generic factors in order to achieve a reliable set of theoretical wavenumbers. This refinement process introduced negligible changes in both the normal mode descriptions and the infrared intensities. Wavenumbers and normal coordinates were calculated by the Wilson FG matrix method.[45]

Results and Discussion

Structural Study. Starting from previous results[20−22] the lowest gas-phase energy gauche and trans conformers at the two tautomeric structures of the imidazole ring were selected as good candidates to begin our search of stationary structures in solution. The trans and gauche conformers of the N^{π} tautomer have been labeled as t1 and g1, respectively, whereas the trans and gauche conformers of the N^{τ} tautomer have been labeled as t3 and g3, respectively. The optimized structures in solution are shown in Figure 2. The trans conformers present a C5C9C12N15 dihedral angle close to 180°, whereas in the gauche conformers this last dihedral angle is lower than 90°.

Some relevant geometrical parameters of the four studied structures optimized in the gas phase and in solution are given in Table 1. For the g1 conformer, the most noticeable change upon solvation is found in the strengthening of the intramolecular hydrogen bond established between the ring nitrogen atom and the amine nitrogen of the tail (N15). This strengthening, reflected in the shorter distances obtained in solution, has been also obtained in the case of the intramolecular hydrogen bond established in the neutral form of glycine in solution and

(27) Richards, W. G.; Wallis, J.; Ganellin, C. R. *Eur. J. Med. Chem.* **1979**, *14*, 9.
(28) Smeyers, Y. G.; Romero-Sánchez, J.; Hernández-Laguna, A. *J. Mol. Struct. (THEOCHEM)* **1985**, *123*, 431.
(29) Paiva, T. B.; Tominaga, M.; Paiva, A. C. M. *J. Med. Chem.* **1970**, *1*, 689.
(30) Rinaldi, D.; Rivail, J. L. *Theor. Chim. Acta* **1973**, *32*, 57.
(31) Rivail, J. L.; Rinaldi, D. *Chem. Phys.* **1976**, *18*, 233.
(32) Rivail, J. L.; Rinaldi, D.; Ruiz-López, M. F. In *Theoretical and Computational Models for Organic Chemistry*; Formosinho, S. J., Arnaut, L., Csizmadia, I., Eds.; Kluwer: Dodrecht, 1991.
(33) Bertrán, J.; Ruiz-López, M. F.; Rinaldi, D.; Rivail, J. L. *Theor. Chim. Acta* **1992**, *84*, 181.
(34) Rinaldi, D.; Rivail, J. L.; Rguini, N. *J. Comput. Chem.* **1992**, *13*, 675.
(35) Peng, C.; Ayala, P. Y.; Schlegel, H. B.; Frish, M. J. *J. Comput. Chem.* **1996**, *17*, 49.
(36) Assfeld, X.; Rinaldi, D. In *AIP Conference Proceedings, ECCC* 1; Bernardi, F., Rivail, J. L., Eds.; AIP Press: Woodbury, NY, 1995; p 59.
(37) Becke, A. D. *Phys. Rev. A* **1988**, *38*, 3098.
(38) Perdew, J. P.; Wang, Y. *Phys. Rev. B* **1992**, *45*, 13244.
(39) Hriharan, P. C.; Pople, J. A. *Theor. Chim. Acta* **1973**, *28*, 213.
(40) Clark, T.; Chandrasekhar, J.; Spitznagel, G. W.; Schleyer, P. V. R. *J. Comput. Chem.* **1983**, *4*, 294.
(41) Frisch, M. J.; Trucks, G. W.; Schlegel, H. B.; Scuseria, G. E.; Robb, M. A.; Cheeseman, J. R.; Zakrzewski, V. G.; Montgomery, J. A., Jr.; Stratmann, R. E.; Burant, J. C.; Dapprich, S.; Millam, J. M.; Daniels, A. D.; Kudin, K. N.; Strain, M. C.; Farkas, O.; Tomasi, J.; Barone, V.; Cossi, M.; Cammi, R.; Mennucci, B.; Pomelli, C.; Adamo, C.; Clifford, S.; Ochterski, J.; Petersson, G. A.; Ayala, P. Y.; Cui, Q.; Morokuma, K.; Malick, D. K.; Rabuck, A. D.; Raghavachari, K.; Foresman, J. B.; Cioslowski, J.; Ortiz, J. V.; Stefanov, B. B.; Liu, G.; Liashenko, A.; Piskorz, P.; Komaromi, I.; Gomperts, R.; Martin, R. L.; Fox, D. J.; Keith, T.; Al-Laham, M. A.; Peng, C. Y.; Nanayakkara, A.; Gonzalez, C.; Challacombe, M.; Gill, P. M. W.; Johnson, B. G.; Chen, W.; Wong, M. W.; Andres, J. L.; Head-Gordon, M.; Replogle, E. S.; Pople, J. A. *Gaussian 98*, revision A.7; Gaussian, Inc.: Pittsburgh, PA, 1998.
(42) Rinaldi, D.; Pappalardo, R. R. *SCRFPAC*; QCPE Indiana University: Bloomington, IN, 1992; Program number 622.
(43) Hickling, S. J.; Wooleey, R. G. *Chem. Phys. Lett.* **1990**, *166*, 43.
(44) Pulay, P.; Fogarasi, G.; Pang, F.; Boggs, J. E. *J. Am. Chem. Soc.* **1979**, *101*, 2550.
(45) Wilson, E. B. *J. Chem. Phys.* **1939**, *7*, 1047.

Table 1. Geometrical Parameters (distances in Å, angles in degrees) and Dipole Moments (in Debyes) for the Four Structures Studied of Neutral Histamine in Solution and Gas Phase

	g1		g3		t3		t1	
	solution	gas phase	solution	gas phase	solution	gas phase	solution	gas phase
N1C5C9C12	−43.85	−43.70	−107.66	−59.26	−78.17	−66.90	−81.58	−70.71
C5C9C12N15	62.733	65.04	59.36	67.21	−179.86	176.53	−176.25	−179.03
C9C12N15H16	−167.57	−171.47	−48.33	−49.84	−58.67	−59.99	−58.30	−57.58
C9C12N15H17	74.75	71.52	63.33	64.78	56.22	57.13	57.38	60.28
N(ring)−H6	1.020	1.015	1.013	1.007	1.010	1.007	1.011	1.008
N15−H16	1.016	1.015	1.017	1.017	1.017	1.016	1.016	1.016
N15−H17	1.017	1.017	1.017	1.018	1.017	1.016	1.017	1.016
N···H	2.096	2.174	3.008	2.340				
N15···N(ring)	2.833	2.878	3.648	3.106				
N15−H···N(ring)	127.32	124.90	121.82	131.14				
μ	7.26	5.70	5.02	4.54	5.15	4.13	5.16	3.57

is a consequence of a solvent induced intramolecular charge separation.[46] An increased electrostatic interaction is thus found between the donor and acceptor hydrogen bond atoms (the Mulliken charges of the hydrogen atom and the N15 atom are increased, in absolute value, from 0.23 and −0.48 au in the gas phase, to 0.29 and −0.56 au in solution, respectively). In the case of the g3 conformer we have noticeable changes in the dihedral angles which describe the relative position of the tail, when passing from vacuum to the continuum. The N1C5C9C12 dihedral angle is increased from −59.26° in the gas phase to −107.66° in solution. In this way the amine group moves away from the imidazole ring plane. This is a solvent-driven change that leads to a weaker intramolecular hydrogen bond with the nitrogen atom of the ring (see the values of the associated distances in Table 1). This is nevertheless compensated with a better solvent exposure and thus with a better intermolecular interaction with the solvent molecules (in this case with the continuum). We have verified that the optimized gas-phase structure is not a stationary structure in solution and, conversely, the in solution optimized structure is not stationary in absence of the continuum. Minor changes are found in the geometrical parameters of t3 and t1 conformers when solvated. The N1C5C9C12 dihedral angle is increased, in absolute value, by about 10 degrees in both cases, the C5C9C12 plane being more perpendicular to the imidazole ring in solution. Table 1 also contains the dipole moments of the four structures in the gas phase and solution. In solution, g3, t1, t3 have similar dipole moments, whereas g1 has the largest value.

Gas phase and aqueous solution relative free energies are given in Table 2. For comparison, we have also included

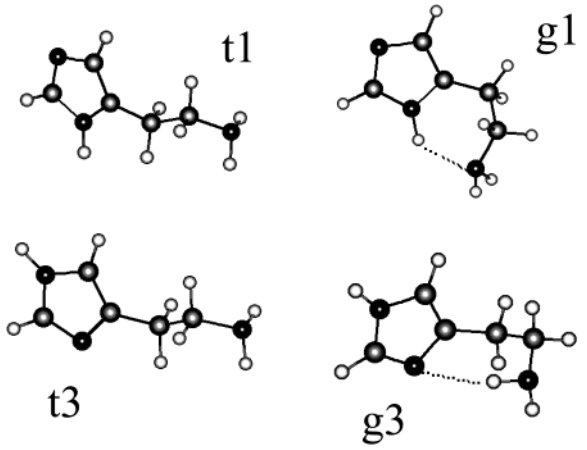

Figure 2. Optimized structures for the four relevant histamine conformers in this work.

Table 2. Relative Free Energies (kcal/mol) for the Studied Structures of Neutral Histamine in the Gas Phase and in Solution

	gas phase		aqueous solution	
structure	B3LYP/6-311G**[a]	MP2/6-311++G**//HF/6-31G*[b]	continuum[a]	Monte Carlo[b]
g1	0.0	0.0	0.0	0.0
g3	1.54	1.80	−1.96	−1.94
t1	3.04	3.20	0.60	−1.28
t3	2.06	2.28	0.15	−3.08

[a] This work. [b] Reference 21.

previously published gas-phase MP2/6-311++G**//HF/6-31G* free energies and the relative free energies obtained from Monte Carlo statistical simulations of the four conformers.[21] Our B3LYP/6-311G** gas-phase free energies are in very good agreement to those of ref 21. The g1 conformer, which present the strongest intramolecular hydrogen bond, is the most stable structure, followed by g3, which also presents an intramolecular hydrogen bond, and finally by t3 and t1. The free energy ordering is completely changed in solution. Monte Carlo simulations, in which the structures were kept frozen to the gas-phase geometry, predicts the t3 conformer as the most stable in solution while our prediction is that g3 is the most stable one. Our result is in agreement with previous continuum model calculations at similar computational levels.[22] Both results, continuum model and statistical simulations agree with the experimental observation that the N^{τ} tautomer predominates in solution,[24] but the experimental technique is not able to distinguish between the trans and gauche conformer. However, we can rationalize the differences found between our results and previously published Monte Carlo free energies in solution. An obvious explanation for this difference is that in these last Monte Carlo calculations the geometry of the neutral histamine was kept frozen at the gas-phase structure, whereas our continuum calculations include the nuclear relaxation under the solvent influence. As said, g3 suffers important geometrical changes upon solvation. In fact, punctual calculation on the g3 structure showed that the gas-phase geometry in solution is 2.9 kcal/mol above the optimized structure. This will explain why the aforementioned simulations do not predict the g3 conformer as the most stable one in solution. In fact, as we have mentioned above, the gas-phase geometry is not an energy minimum in solution. There is an additional difference between our results and those obtained from the Monte Carlo simulations: the overestabilization of the trans conformers with respect to the

(46) Tortonda, F. R.; Pascual-Ahuir, J. L.; Silla, E.; Tuñón, I.; Ramírez, F. J. *J. Chem. Phys.* **1998**, *109*, 592.

Table 3. Atomic Charges (in au) for T3 Structure of Neutral Histamine in Solution

atom	CHELP[a]	Mulliken[a]	MM potential[b]
N1	−0.66	−0.37	−0.49
C2[c]	0.35	0.27	0.41
N3	−0.20	−0.33	−0.57
C4[c]	−0.15	0.16	0.13
C5	0.50	−0.05	0.10
H(N3)	0.30	0.27	0.42
C12[c]	−0.38	0.02	0.00
C9[c]	0.61	0.13	0.25
N15	−1.08	−0.51	−1.05
H(N15)	0.36	0.20	0.40

[a] This work. [b] Reference 21. [c] Aliphatic hydrogen charges are summed up to the carbon charges.

gauche in this last kind of calculations. In this case, the difference can be due to the set of atomic charges of the intermolecular potential used in the simulations. Table 3 shows these charges (which are the same for all the conformers/tautomers) together with the Mulliken and CHELP[47] charges obtained from our solution wave function of structure t3. Although the imidazole ring, C12 and C9 charges of the potential function employed in the simulation are close to the Mulliken values, the charges of the amine nitrogen and hydrogen atoms are closer to the CHELP charges. These charges are larger, in absolute value, than the Mulliken atomic charges. Thus, we believe that the charges used in the intermolecular potential function could favor the trans conformation, where the amine group is more exposed to solvent interactions. In fact, the authors pointed out that the charges of the amine group and the rest of the molecule were taken from different potentials.[21] Obviously, the difference between conformers/tautomers is so subtle that other effects, which have been not fully explored in our present continuum calculations, cannot be discarded as possible error sources. However, we believe that our results, which predict the gauche conformers as more stable in solution than the trans ones, are reliable. In particular, we propose g3 conformer as the most populated structure in solution and thus the best candidate, from an energetic point of view, to compare the theoretical and experimental vibrational spectra.

It is also worth to mention the different dipole moments found for the g1 and g3 structures, which are those structures predicted as the most stable in solution. This can be important in order to analyze the observed vibrational spectra, as far as it can result in very different intensities. One could ask why being g1 the most stable structure in the gas phase and the structure with the largest dipole moment, this is not the most stable structure in solution. The reason is found in higher-order multipole contributions to the solvation free energy. In particular, the dipole/quadrupole contributions to the solvation free energy of g1 and g3 are $-5.01/-0.97$ kcalmol^{-1} and $-3.05/-6.01$ kcal/mol, respectively.

Although the prevalence of the g3 conformer has been established in terms of nonespecific solvent effects, this structure could be also stabilized by means of a bifunctional water molecule. Using the same computational level, we have localized a minimum energy structure for the a complex of a water molecule and g3, where the water molecule forms two hydrogen bonds with histamine: it acts as proton donor with the nitrogen atom of the ring (the N1···H(water) distance being 1.942 Å) and as proton acceptor with the NH_2 group (the O(water)···H17 distance being 2.217 Å). Bifunctional water molecules are known to play an important role stabilizing molecular structures in solution,[48] most probably due to hydrogen bond cooperative effects. In this complex, the geometry of the g3 conformer remains essentially the same as found in the continuum model. Interestingly, the free hydrogen atom of the amine group, the one that does not interact with the water molecule, is still oriented toward the nitrogen atom of the ring, being the N1···H16 distance 2.782 Å, in between of the values obtained for the gas phase and in solution optimizations of the histamine g3 conformer. The optimized geometry of the g3-water complex is given as Supporting Information. As a further test for the stability of g3 structure in aqueous solution, we have run an AM1/TIP3P NVT molecular dynamics simulation at 300 K with 1027 classical water molecules using DYNAMO.[49] The system was equilibrated during 30 ps constraining the N1···H16 distance to 2.8 Å. After this, the constraint was removed and we carried out 20 ps of production during which neutral histamine always kept the geometry of g3 conformer. The N1−H16 distance ranged between 2.2 and 3.4 Å with a mean value of 2.82 ± 0.28 Å.

Infrared and Raman Spectra. We have computed harmonic force fields for the histamine tautomers studied. To compare the predicted vibrational spectra with the experimental results, we need a reliable assignment of the histamine infrared and Raman spectra in solution. The FT-IR and FT-Raman spectra of neutral histamine in H_2O and D_2O are displayed in Figure 3. The observed wavenumbers, relative intensities and proposed assignments are summarized in Table 4 for natural histamine and its N-deuterated derivative. The assignments were referred to commonly used locally symmetrized vibrational modes,[50] which can be easily correlated with characteristic group wavenumbers. Main criteria for assignments were the isotopic shifts upon deuteration and correlations with previous vibrational studies in solution on histamine species.[17,18] Results from the normal mode calculations were only used when the experimental data are not able to discriminate among putative assignments, which largely happened in the spectral region below 1000 cm^{-1}.

The $\nu(CH_2)$ and $\nu(CH)$ wavenumbers measured for histamine free-base in solution can be compared with those reported for histamine monocation.[17] Thus, while maximal deviation for the imidazole C−H stretching modes was 13 cm^{-1} (0.4%), the methylene wavenumbers were significantly higher for the monocation than for the free-base. This fact evidences the structural similarities between the corresponding aromatic rings, as aforementioned, whereas the different charge distributions of the side-chains give rise to rather different wavenumbers for the methylene stretching vibrations. A similar comparison can be also achieved from the vibrational spectra of solid histamine free-base[51] and histamine monohydrochloride.[16]

The Raman spectrum of neutral histamine in H_2O solution, Figure 3, showed two close bands around 1580 cm^{-1}, which have been confirmed in the corresponding infrared spectrum. The one at lower intensity, namely at 1587 cm^{-1}, did not appear

(47) Chirlian, L. E.; Francl, M. M. *J. Comput. Chem.* **1987**, *5*, 129.
(48) Carlson, H. A.; Jorgensen, W. L. *J. Am. Chem. Soc.* **1996**, *118*, 8475.
(49) Field, M. J.; Albe, M.; Bret, C.; Proust-de Martin, F.; Thomas, A. *J. Comput. Chem.* **2000**, *21*, 1088.
(50) Wilson, E. B.; Decius, J. C.; Cross, P. C. *Molecular Vibrations*; McGraw-Hill: New York, 1955.
(51) Bellocq, A. N.; Garrigou-Lagrange, C. *J. Chim. Phys. Physicochim. Biol.* **1970**, *67*, 1544.

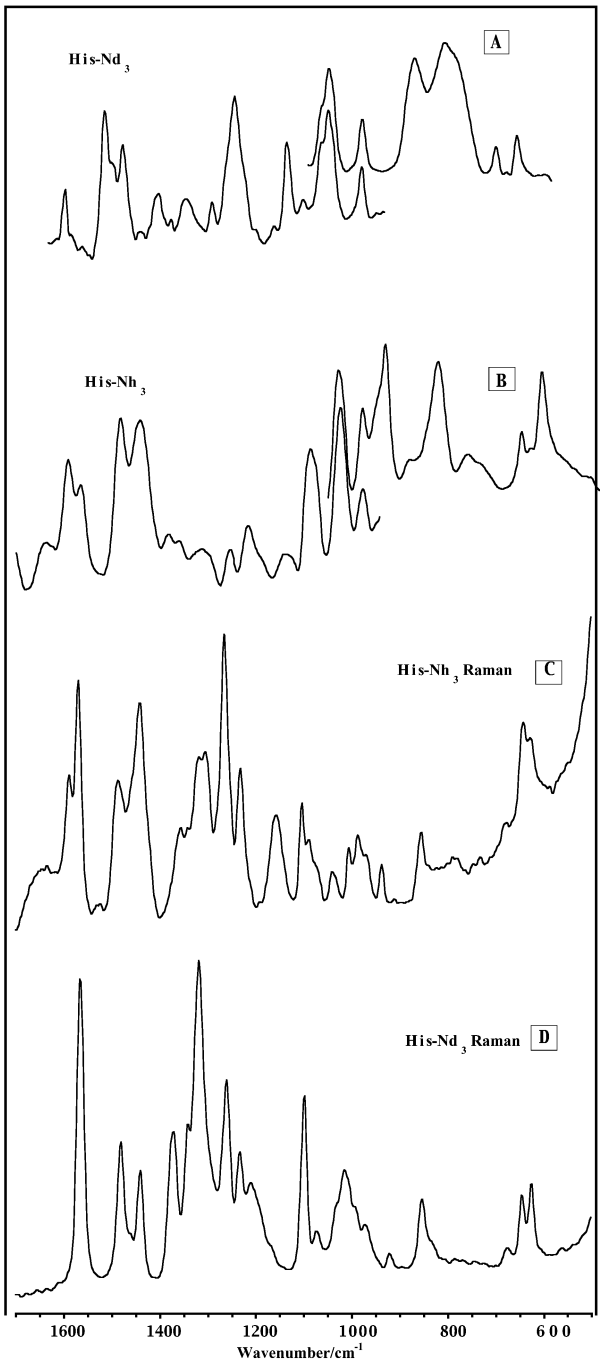

Figure 3. Fourier transform vibrational spectra of neutral histamine in solution between 1700 and 500 cm^{-1}. A. Infrared spectrum in D_2O. B. Infrared spectrum in H_2O. C. Raman spectrum in H_2O. D. Raman spectrum in D_2O.

when changing H_2O by D_2O in both infrared and Raman spectra, being consequently assigned to the NH_2 bending vibration, $\delta(NH_2)$. The corresponding $\delta(ND_2)$ mode was assigned to the band at 1209 cm^{-1} measured in the Raman spectrum of the D_2O solution, which was not observed in H_2O. The band at 1570 cm^{-1} shifted downward by 5 cm^{-1} when deuteration. This small deviation is characteristic of an imidazole ring stretching mode, ν(ring).[16−18] Taking into account the structural similarities between the aromatic moieties of neutral histamine and the monocation, as aforementioned, we can also expect some correlations between the related vibrational frequencies. The imidazole stretching vibration of histamine monocation appearing at the highest wavenumber was measured at 1574 cm^{-1}. It shifted by −6 cm^{-1} upon deuteration,[17] which support the present assignment. The small shift measured for this mode also indicates some contribution from the N−H bending vibration, δ(NH), in the related normal mode.

Strong absorptions at 1489, 1451, and 1439 cm^{-1} were measured in the infrared spectrum of neutral histamine in H_2O solution between 1400 and 1500 cm^{-1}. They were observed at 1486, 1452, and 1442 cm^{-1} in the Raman spectrum. The infrared spectra in D_2O solution showed bands at 1483, 1462 and 1445 cm^{-1}, together with a new band at 1371 cm^{-1}, all of them confirmed by Raman spectroscopy. Putative assignments for these bands involve two imidazole ring stretching modes, ν(ring), and two methylene bending vibrations, $\delta(CH_2)$. Experimental and theoretical results on histamine monohydrochloride[17] reported isotopic shifts of −12 and −55 cm^{-1} for the two ν(ring) modes in this region, as a consequence of coupling with vibrational coordinates involving N−H bonds. Because the structural similarities of the imidazole moieties from both the free-base and the monocation, the pair of bands at 1489, 1451 cm^{-1} in H_2O, and 1483, 1371 in D_2O, were assigned to the imidazole stretching modes. Deviations when deuteration of −5 and −79 cm^{-1} are consistent with those measured for histamine monocation. Methylene bending vibrations were measured at 1439 and 1442 cm^{-1} in H_2O, and 1445 and 1440 cm^{-1} in D_2O, all of them within the expected range of appearing for these modes.[51]

The two remaining imidazole stretching vibrations were assigned to the relatively intense Raman bands at 1309 and 1267 cm^{-1}. The former band was not observed in D_2O. By correlating with histamine monocation we do not expect a major shift for it when deuteration, so it should be hidden behind the strong band at 1319 cm^{-1}, which was assigned to a methylene twisting vibration. The second ν(ring) band shifted downward by 5−6 cm^{-1}, which is in the expected range for this mode. These Raman wavenumbers were all confirmed in the infrared spectra.

The rest of bands measured between 1400 and 1300 cm^{-1} have been assigned to the methylene wagging and twisting vibrations. Below 1300 cm^{-1}, the imidazole N−H in-plane bending and the amine rocking modes are expected to appear at near wavenumbers.[52] They were both assigned to the broad Raman band centered at 1160 cm^{-1}, which was not observed for solutions in D_2O. It was correlated to the infrared absorption at 1150 cm^{-1}. Upon deuteration, they were assigned at 947 cm^{-1} (ND_2 rocking) and 835 cm^{-1} (imidazole N−D in-plane bending). This splitting respect to the solution in natural water can be explained from the involved normal modes. Thus, a significant coupling of the N−D in-plane vibration with imidazole stretching and bending vibrations is usually expected. This fact would give rise to a smaller shift for δ(N−D) than for r(ND_2), as observed.

Correlations with histamine monocation[17] leaded us to assign the two imidazole C−H in-plane bending modes to the Raman bands at 1232 and 1105 cm^{-1}, which exhibited small shifts when deuteration. Assignments between 1100 and 900 cm^{-1} were largely related to imidazole ring in-plane bending and the side-chain skeletal vibrations, which are expected widely mixed. Contributions from amine vibrations are also probable, what

(52) Roeges, N. P. G. *A Guide to the Complete Interpretation of Infrared Spectra of Organic Structures*; John Wiley and Sons: Chichester, 1994.

Table 4. Wavenumbers,[a] Relative Intensities,[b] and Proposed Assignments of the Infrared and Raman Bands of Neutral Histamine in Aqueous Solution

histamine–Nh_3				histamine–Nd_3				
infrared		Raman		infrared		Raman		
ν	rel.int.	$\Delta\nu$	rel.int.	ν	rel.int.	$\Delta\nu$	rel.int.	assignments
		3362	sh					amine stretching
		3304	sh					amine stretching
		3148	w	3143	sh	3148	m	imidazole C−H stretching
		3132	m	3131	m	3131	m−s	imidazole C−H stretching
		2942	m	2950	vs	2948	sh	methylene stretching
		2926	m			2928	s	methylene stretching
		2888	w	2884	s	2886	m	methylene stretching
		2856	w	2853	sh	2856	m	methylene stretching
1596	s	1587	m					NH_2 scissoring
1570	m	1570	s	1565	m	1565	s	imidazole ring stretching
1489	s	1486	m	1483	s	1481	m	imidazole ring stretching
1451	s	1452	sh					imidazole ring stretching
1439	s	1442	s	1445	m−s	1440	m	methylene scissoring
				1371	m	1372	m	imidazole ring stretching
1363	w	1358	w	1345	w−m	1341	m	methylene wagging
1339	w	1340	sh					methylene wagging
1320	w	1322	m−s	1317	w−m	1319	vs	methylene twisting
1308	sh	1309	m−s					imidazole ring stretching
1265	w−m	1267	vs	1260	w−m	1261	m−s	imidazole ring stretching
1225	m	1232	m	1226	sh	1232	m	imidazole C−H in-plane bending
				1211	s	1209	w−m	ND_2 scissoring
1150	w	1160	m					im. N−H in-pl. bend., NH_2 rock.
1103	s	1105	m	1103	m−s	1098	m−s	imidazole C−H in-plane bending
1086	m	1091	w−m	1069	w	1073	w	side-chain skeletal stretching
1037	s	1037	w	1017	s	1015	m	side-chain skeletal stretching
1007	w	1006	w−m					side-chain skeletal stretching
988	m	989	m			972	w−m	imidazole ring in-plane bending
				947	m			ND_2 rocking
939	s	938	w−m	920	w	921	w	imidazole ring in-plane bending
		906	w					NH_2 wagging
		856	m	852	sh	853	m	methylene rocking
				834	s	835	sh	N−D in-plane bending
834	s							imidazole C−H out-pl. bending
		804	w			806	vw	imidazole C−H out-pl. bending
				779	vs	785	vw	ND_2 wagging
772	w	778	w	763	sh	769	vw	methylene rocking
		705	w	669	w−m	675	w	side-chain skeletal bending
643	m	644	m	645	w	645	m	imidazole ring out-plane bending
623	s	628	m	622	m	626	m	imidazole ring out-plane bending
		604	w					imidazole N−H out-pl. bending
						491	w	imidazole N−D out-pl. bending
		384	m			367	m	side-chain skeletal bending

[a] Wavenumbers in cm^{-1}. [b] s = strong; m = medium; w = weak; v = very; sh = shoulder.

would justify the moderate isotopic shifts upon deuteration measured for the most of bands in this region. This behavior is commonly observed for the Raman bands measured below 900 cm^{-1}, which has been mainly assigned to methylene rocking, r(CH_2), and imidazole out-of-plane bending, γ(ring), vibrations. A last amine vibration, $\omega(NH_2)$, was measured at 906 cm^{-1} in H_2O and 779 cm^{-1} in D_2O, whereas the imidazole γ(N−H) mode was assigned to the Raman band at 604 cm^{-1}, which disappears when deuteration. It was tentatively assigned to the 491 cm^{-1} band in D_2O.

The Raman spectra of the two cationic histamine species in water solution exhibited a couple of bands between 600 and 650 cm^{-1} which were both assigned to imidazole ring out-of-plane bending modes.[17,18] For neutral histamine, these bands have been measured at 644 and 628 cm^{-1}, both confirmed in the infrared spectrum. They deviate ±2 cm^{-1} respect to those measured for histamine monocation,[17] in contrast with a mean difference of about −20 cm^{-1} measured for histamine dication.[18] This fact arises from the presence of a second hydrogen atom attached to the imidazole ring. It also confirms that the relevant tautomer for histamine monocation in water solution is $[C_3N_2H_3-CH_2CH_2NH_3]^+$, instead $[C_3N_2H_4-CH_2CH_2NH_2]^+$; the positive net charge is nevertheless shared by both the aromatic and the aliphatic moieties, as demonstrated from density functional calculations.[17] Skeletal bending and torsional vibrations usually appear at wavenumbers lower that 600 cm^{-1}, so they have not been measured in this work, with the exception of a medium intensity band measured at 384 and 367 cm^{-1}, in H_2O and D_2O, respectively.

Vibrational Dynamics. The first step of this section was to extend the conformational analysis of histamine free base to vibrational features. A quadratic force field for each tautomer was calculated from the second derivatives of the molecular energy, in Cartesian coordinates, at the minimal energy geometry. To achieve a normal modes description in term of vibrational coordinates, the Cartesian force constants were transformed into the set of nonredundant locally symmetrized internal coordinates summarized in Table 5, which allowed us for a suitable comparison among the four sets of wavenumbers. Table 6 lists the calculated values for the stretching and bending

Table 5. Locally Symmetrized Internal Coordinates Used in This Work for Neutral Histamine

n°	coordinate[a]	symbol	description
1	$r_{1\,2}$	ν (ring)	ring stretching
2	$r_{2\,3}$	ν(ring)	ring stretching
3	$r_{3\,6}$	ν(NH)	N−H stretching
4	$r_{3\,4}$	ν(ring)	ring stretching
5	$r_{2\,7}$	ν(CH)	C−H stretching
6	$r_{4\,5}$	ν(ring)	ring stretching
7	$r_{5\,1}$	ν(ring)	ring stretching
8	$r_{4\,8}$	ν(CH)	C−H stretching
9	$r_{5\,9}$	ν(CX)	side chain stretching
10	$2^{-1/2}\,(r_{9\,10} + r_{9\,11})$	ν_s (CH_2)	CH_2sym. stretching
11	$2^{-1/2}\,(r_{9\,10} - r_{9\,11})$	ν_a (CH_2)	CH_2antisym. stretch.
12	$r_{9\,12}$	ν(side chain)	side chain stretching
13	$2^{-1/2}\,(r_{12\,13} + r_{12\,14})$	ν_s (CH_2)	CH_2sym. stretching
14	$2^{-1/2}\,(r_{12\,13} - r_{12\,14})$	ν_a (CH_2)	CH_2antisym. stretch.
15	$r_{12\,15}$	ν(side chain)	side chain stretching
16	$2^{-1/2}\,(r_{15\,16} + r_{15\,17})$	ν_s (NH_2)	NH_2sym. stretching
17	$2^{-1/2}\,(r_{15\,16} - r_{15\,17})$	ν_a (NH_2)	NH_2antisym. stretch.
18	$0.6324\beta_{2\,1\,5} - 0.5116(\beta_{1\,2\,3}+\beta_{1\,5\,4}) + 0.19543(\beta_{2\,3\,4}+\beta_{3\,4\,5})$	δ (ring)	ring in-plane bending
19	$0.3717\,(\beta_{3\,2\,1} - \beta_{3\,4\,5}) + 0.6015\,(\beta_{2\,1\,5} - \beta_{1\,5\,4})$	δ (ring)	ring in-plane bending
20	$2^{-1/2}\,(\beta_{1\,2\,7} - \beta_{3\,2\,7})$	δ (CH)	CH in plane bending
21	$2^{-1/2}\,(\beta_{4\,3\,6} - \beta_{2\,3\,6})$	δ (NH)	NH in plane bending
22	$2^{-1/2}\,(\beta_{1\,5\,9} - \beta_{4\,5})$	δ (CX)	side chain in-pl bend.
23	$2^{-1/2}\,(\beta_{5\,4\,8} - \beta_{3\,4\,8})$	δ (CH)	CH in plane bending
24	$26^{-1/2}\,(5\beta_{10\,9\,11} + \beta_{5\,9\,12})$	δ (CH_2)	CH_2bending
25	$26^{-1/2}\,(5\beta_{5\,9\,12} + \beta_{10\,9\,11})$	δ (side chain)	side chain bending
26	$1/2\,(\beta_{12\,9\,10} + \beta_{12\,9\,11} - \beta_{5\,9\,10} - \beta_{5\,9\,11})$	ω (CH_2)	CH_2wagging
27	$1/2\,(\beta_{12\,9\,10} - \beta_{12\,9\,11} - \beta_{5\,9\,10} + \beta_{5\,9\,11})$	t (CH_2)	CH_2twisting
28	$1/2\,(\beta_{12\,9\,10} - \beta_{12\,9\,11} + \beta_{5\,9\,10} - \beta_{5\,9\,11})$	r (CH_2)	CH_2rocking
29	$26^{-1/2}\,(5\beta_{13\,12\,14} + \beta_{9\,12\,15})$	δ (CH_2)	CH_2bending
30	$26^{-1/2}\,(5\beta_{9\,12\,15} + \beta_{13\,12\,14})$	δ side chain)	side chain bending
31	$1/2\,(\beta_{15\,12\,13} + \beta_{15\,12\,14} - \beta_{9\,12\,13} - \beta_{9\,12\,14})$	ω (CH_2)	CH_2wagging
32	$1/2\,(\beta_{15\,12\,13} - \beta_{15\,12\,14} - \beta_{9\,12\,13} + \beta_{9\,12\,14})$	t (CH_2)	CH_2twisting
33	$1/2\,(\beta_{15\,12\,13} - \beta_{15\,12\,14} + \beta_{9\,12\,13} - \beta_{9\,12\,14})$	r (CH_2)	CH_2rocking
34	$6^{-1/2}\,(2\beta_{16\,15\,17} - \beta_{12\,15\,16} - \beta_{12\,15\,17})$	δ (NH_2)	NH_2bending
35	$2^{-1/2}\,(\beta_{12\,15\,16} - \beta_{12\,15\,17})$	r (NH_2)	NH_2rocking
36	ϕ_{15}	ω (NH_2)	NH_2wagging
37	ϕ_3	γ (NH)	NH out-pl bending
38	ϕ_2	γ (CH)	CH out-pl bending
39	ϕ_4	γ (CH)	CH out-pl bending
40	ϕ_5	γ (CX)	side chain out-pl bend
41	$0.6324\,\tau_{1\,5} - 0.5116\,(\tau_{3\,2}+\tau_{4\,5}) + 0.1954\,(\tau_{1\,5}+\tau_{1\,2})$	γ (ring)	ring out-pl bending
42	$0.3717\,(\tau_{4\,5} - \tau_{3\,2}) + 0.6015\,(\tau_{1\,2} - \tau_{1\,5})$	γ (ring)	ring out-pl bending
43	$\tau_{5\,9}$	τ (CX)	side chain torsion
44	$\tau_{9\,12}$	τ (side chain)	side chain torsion
45	$\tau_{12\,15}$	τ (NH_2)	side chain torsion

[a] See Figure 1 for atomic numbering; r_{ij} is the stretching vibrations of the bond between atoms i and j; β_{ijk} is the vibration of the angle between atoms i, j, and k; ϕ_i is the out-of-plane vibration of the atom i; τ_{ij} is the torsion vibration with respect to the bond between atoms i and j.

Table 6. Theoretical Wavenumbers (in cm^{-1}) and Assignments Obtained for Selected Imidazole Vibrations of the Four Structures Studied of Neutral Histamine in Solution

exp.	g1	g3	t3	t1	assignments
1570	1578 (+8)	1557 (−13)	1564 (−6)	1580 (+10)	imidazole ring stretching
1489	1478 (−11)	1492 (+6)	1494 (+5)	1477 (−1)	imidazole ring stretching
1451	1404 (−46)	1441 (−10)	1439 (−12)	1410 (−41)	imidazole ring stretching
1309	1358 (+47)	1320 (+11)	1327 (+16)	1359 (+50)	imidazole ring stretching
1265	1266 (+2)	1262 (−3)	1251 (−14)	1226 (−39)	imidazole ring stretching
989	1006 (+17)	971 (−18)	970 (−19)	1000 (+11)	imid. ring in-plane bending
939	930 (−9)	931 (−8)	932 (−7)	923 (−16)	imid. ring in-plane bending
644	687 (+43)	670 (+26)	687 (+43)	670 (+26)	imid. ring out-plane bending
628	657 (+29)	630 (+2)	650 (+22)	660 (+32)	imid. ring out-plane bending

Wavenumbers were uniformly scaled by a factor of 0.97 applied to the quadratic force fields. Differences between experimental and calculated wavenumbers are given in parenthesis.

imidazole ring vibrations, which were uniformly scaled by a generic factor of 0.97 applied to all the force constants,[53] and their deviations respect to the experimental wavenumbers. Imidazole vibrations were selected since they have significant contributions from the histamine polar groups, which are strongly involved in the interaction with the solvent molecules; they are, therefore, good representatives of the histamine free-

(53) National Institute of Standards and Technology, NIST. Computational chemistry comparison and benchmark database. Update **2002**, III. C.1: Vibrational scale factors.

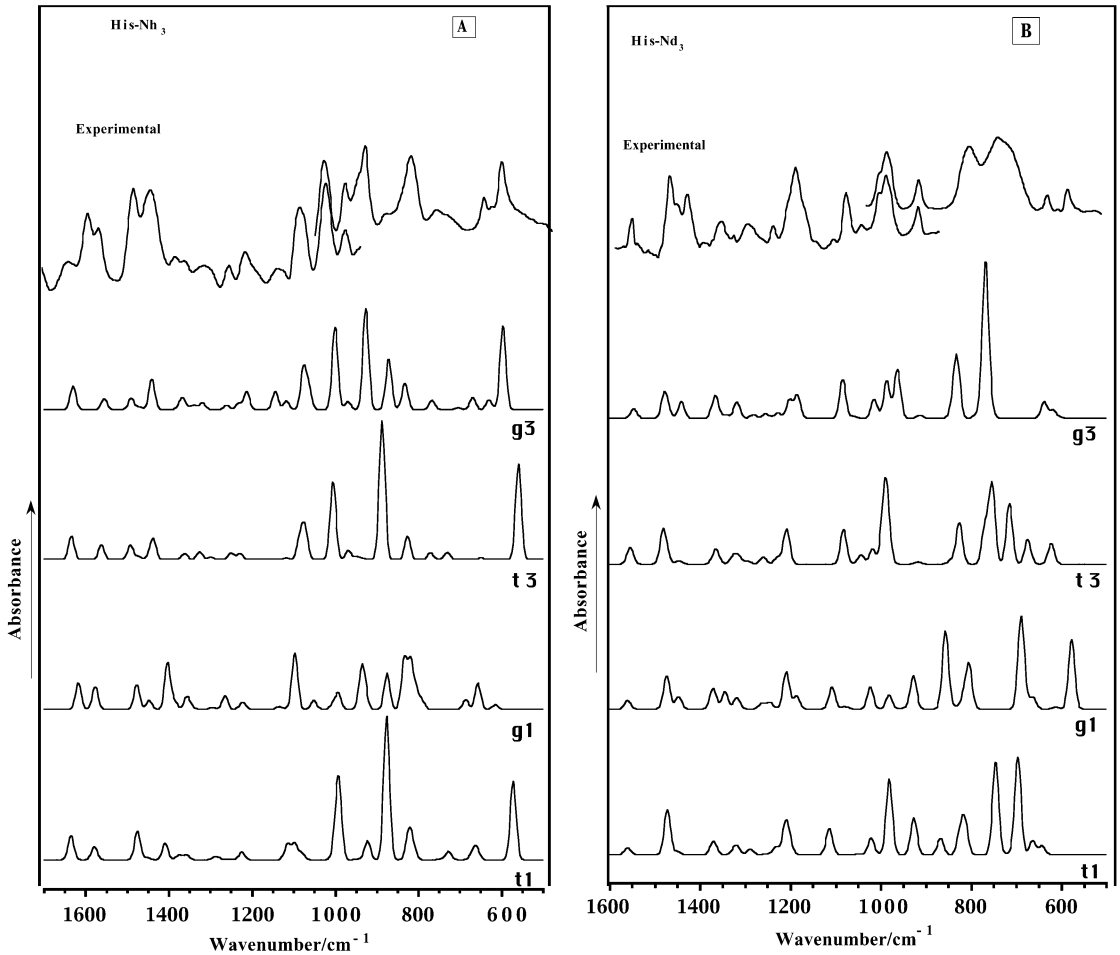

Figure 4. Theoretical SCRF/6-311G** infrared spectra obtained for the four structures studied of neutral histamine in solution. The experimental infrared spectra were included for comparing. A. Natural derivative. B. Deuterated derivative.

base vibrations. Obtained quadratic mean deviations were 29.0, 12.9, 19.4, and 29.6 cm^{-1} for g1, g3, t3, and t1, respectively, which confirms the g3 tautomer as the relevant structure. It is also interesting to analyze the obtained differences between experimental and theoretical values. The imidazole stretching wavenumber measured at 1451 cm^{-1} is better evaluated for N^{τ} than for N^{π} tautomers, whereas the band at 1265 cm^{-1} discriminates between gauche and trans structures. The calculated potential energy distributions assigned the former wavenumber to a ring stretching mode with participation (30%) of the imidazole N−H in-plane bending vibration, while the second wavenumber was assigned to a ring stretching mode with relevant contributions (42%) of methylene twisting and wagging vibrations from the side chain. These results suggest that the gauche tautomers (g1 and g3) better reproduce side chain vibrations, whereas the N^{τ} tautomers (g3 and t3) better reproduce imidazole vibrations, thus indicating the g3 tautomer as the relevant structure of neutral histamine in solution. Deviations for the imidazole bending vibrations were similar for the four tautomers, with the exception of the out-of-plane bending vibrations measured at 628 cm^{-1}. This wavenumber only was successfully predicted by the g3 structure, which supports our conclusion. Its related potential energy distribution also showed significant contributions from side chain vibrations, contrarily to the other three imidazole bending vibrations, whose normal modes showed negligible contributions from other coordinates. The imidazole ring vibrations have thus allowed to evaluate the reliability of the four histamine conformers by means of their interactions with different vibrational coordinates. Two main trends were observed. The imidazole vibrations widely coupled to side chain vibrations were better predicted for the g3 tautomer, while those scarcely mixed were similarly predicted by the four structures studied, although the N^{τ} conformers always obtained wavenumbers closer to the experimental values.

Calculated infrared intensities were also compared with those experimental. Figure 4 shows the theoretical infrared spectra for the four histamine conformers studied. The observed infrared spectra were included for comparing. They were designed from pure ab initio intensities in combination with uniformly scaled (by 0.97) wavenumbers. As a general trend, the theoretical spectra for the g3 structure exhibited the best fitting to the experimental infrared spectra. Concerning the natural derivative, Figure 4a, noticeable differences among the four calculated spectra were observed between 1200 and 800 cm^{-1}. The intensity of the medium or strong bands measured at 1103, 1086, 1037, and 939 cm^{-1}, Figure 3b, were successfully predicted at 1076, 1063, 1001, and 931 cm^{-1} for the g3 conformer. The theoretical spectrum for the t3 conformer showed a similar pattern than the g3 one over the whole spectral region, except between 1000 and 800 cm^{-1}, where a very intense absorption was predicted at 888 cm^{-1}. This fact was also observed for the t1 conformer, while the g1 one exhibited the greater deviations from the experimental infrared spectrum. These trends were supported by the theoretical spectra for N-deuterated histamine,

Table 7. B3LYP/6-311G** Vibrational Wavenumbers (in cm^{-1}) and Normal Mode Descriptions for Neutral Histamine-Nh_3 in Aqueous Solution

vibr.[a]	calculated	experim. infrared	experim. Raman	potential energy distribution (greater than 10%)[b]
ν_1	3469			100 ν(NH)
ν_2	3367		3362	100 $\nu_a(NH_2)$
ν_3	3310		3304	100 $\nu_s(NH_2)$
ν_4	3156		3148	99 ν(CH)
ν_5	3127		3132	100 ν(CH)
ν_6	2941		2942	97 $\nu_a(CH_2)$
ν_7	2919		2926	86 $\nu_a(CH_2)$ + 14 $\nu_s(CH_2)$
ν_8	2901		2888	97 $\nu_s(CH_2)$
ν_9	2867		2856	85 $\nu_s(CH_2)$ + 15 $\nu_a(CH_2)$
ν_{10}	1607	1596	1587	100 $\delta(NH_2)$
ν_{11}	1552	1570	1570	64 ν (ring) + 14 ν(CX) + 13 δ(CH)
ν_{12}	1483	1489	1486	60 ν(ring) + 33 δ(CH) + 10 δ(NH)
ν_{13}	1448		1442	100 $\delta(CH_2)$
ν_{14}	1432	1451	1452	56 ν(ring) + 30 δ(NH) + 14 δ(ring)
ν_{15}	1422	1439		100 $\delta(CH_2)$
ν_{16}	1353	1363	1358	34 $\omega(CH_2)$ + 28 t(CH_2) + 19 r(NH_2)
ν_{17}	1345	1339	1340	57 $\omega(CH_2)$ +24 t(CH_2)
ν_{18}	1328	1320	1322	45 ν(ring) + 30 $\omega(CH_2)$ + 13 t(CH_2)
ν_{19}	1313	1308	1309	48 ν(ring) + 28 $\omega(CH_2)$ + 10 δ(CH)
ν_{20}	1251	1265	1267	30 ν(ring) + 27 $\omega(CH_2)$ + 15 t(CH_2)
ν_{21}	1223	1225	1232	53 δ(CH) + 32 ν(ring)
ν_{22}	1200		1196	30 t(CH_2) + 12 r(CH_2) + 12 δ(CH) + 10 ν(ring)
ν_{23}	1133	1150	1160	31 t(CH_2) + 19 r(NH_2) + 16 ν(side chain) + 12 $\omega(NH_2)$
ν_{24}	1112	1103	1105	49 ν(ring) + 25 δ(NH)
ν_{25}	1071	1086	1091	42 ν(ring) + 26 δ(CH) + 10 δ(NH)
ν_{26}	1054	1037	1037	32 t(CH_2) + 17 ν(ring) + 17 $\omega(NH_2)$ + 16 ν(side chain)
ν_{27}	998	1007	1006	69 ν(side chain) + 17 $\omega(NH_2)$
ν_{28}	968	988	989	43 δ(ring) + 27 ν(ring)
ν_{29}	931	939	938	77 δ(ring)
ν_{30}	917		906	38 $\omega(NH_2)$ + 35 r(CH_2) + 17 ν(side chain) + 11 r(NH_2)
ν_{31}	865		856	33 r(CH_2) + 18 $\omega(NH_2)$ + 23 ν(side chain) + 13 δ(ring)
ν_{32}	841	834		57 γ(CH) + 32 γ(ring)+ 11 ν(side chain)
ν_{33}	831		804	42 γ(CH) + 25 ν(side chain) + 22 r(CH_2) + 11 γ(ring)
ν_{34}	768	772	778	75 γ(CH) + 25 γ(ring)
ν_{35}	704		705	47 γ(ring) + 23 γ(CX) + 13 r(CH_2)
ν_{36}	671	643	644	83 γ(ring) + 17 γ(NH)
ν_{37}	630	623	628	30 ν(CX) + 21 δ(ring) + 11 γ(ring)
ν_{38}	598		604	100 γ(NH)
ν_{39}	467			58 δ(side chain) + 11 r(CH_2)
ν_{40}	357		384	39 δ(CX)+21τ(side chain)+14$\tau(NH_2)$+14δ(side chain)+12 r(CH_2)
ν_{41}	314			75 $\tau(NH_2)$ + 22 δ(CX)
ν_{42}	284			48 δ(side chain) + 29 γ(ring) + 18 γ(CX)
ν_{43}	168			28 δ(side chain) + 27 τ(side chain) + 20 γ(CX) + 12 δ(CX)
ν_{44}	103			50 τ(side chain) + 14 γ(CX) + 12 δ(side chain)
ν_{45}	59			100 τ(CX)

[a] Arbitrary numbering. [b] Symbols correspond to the coordinates listed in Table 5; coordinates with similar characters were added to clarify.

Figure 4b. A reliable prediction of the experimental infrared spectrum, Figure 3a, was achieved for the g3 conformer. The experimental wavenumbers 1103 (s), 1069 (w), 1017 (s), 947 (m), 838 (s), and 779 (s), can be well correlated with the g3 wavenumbers 1084, 1061, 1013, 964, 833, and 768 cm^{-1}, in the basis of their calculated infrared intensities. The observed-calculated adjust was also quite correct for the t3 structure, although the predicted strong absorptions at 990 and 716 cm^{-1} cannot be successfully correlated to experimental bands. The calculated spectra for both the g1 and t1 conformers exhibited greater deviations than for the natural derivative. In summary, the infrared intensity comparison agrees with the aforementioned results for the wavenumbers. As a general rule, the experimental intensities were better predicted for N^{τ} than for N^{π} conformers of neutral histamine in solution. This means that the position of the nitrogen-attached hydrogen atom of the imidazole ring has a greater influence on the infrared intensities than the relative conformation of the side-chain respect to the aromatic moiety. Concerning the two N^{τ} tautomers, better results were obtained for the g3 structure.

As the final step of this work, we have improved the force field obtained for the g3 tautomer by a scaling procedure. To preserve the essence of the theoretical approach, we have used only two generic scaling factors: 0.97 for the coordinates involving weight atoms and 0.94 for the coordinates involving hydrogen atoms. Exception was made for the methylene and amino stretching coordinates, for which a particular factor of 0.91 was applied since they are very local and undoubtedly assigned modes. This methodology was successfully employed for histamine monocation.[17] The scaled wavenumbers and normal coordinate descriptions are summarized in Tables 7 and 8 for the natural and N-deuterated derivative, respectively. Diagonal force constants are listed in Table 9. Off-diagonal terms of the quadratic force field are given as Supporting Information.

The scaled theoretical wavenumbers exhibit a good fitting to the experimental values for both the natural and the N-deuterated molecules. Deviations were lower than 10 cm^{-1} (in absolute value) for most of the wavenumbers, as can be seen in Tables 7 and 8. On the other hand, normal mode descriptions

Table 8. B3LYP/6-311G** Vibrational Wavenumbers (in cm^{-1}) and Normal Mode Descriptions for Neutral Histamine-Nd_3 in Aqueous Solution

vibr.[a]	calculated	experim. infrared	experim. Raman	potential energy distribution (greater than 10%)[b]
ν_1	3157	3143	3148	99 ν(CH)
ν_2	3127	3131	3131	100 ν(CH)
ν_3	2941	2950	2948	97 $\nu_a(CH_2)$
ν_4	2919		2928	85 $\nu_a(CH_2)$ + 15 $\nu_s(CH_2)$
ν_5	2901	2884	2886	97 $\nu_s(CH_2)$
ν_6	2867	2853	2856	85 $\nu_s(CH_2)$ + 15 $\nu_a(CH_2)$
ν_7	2553			98 ν(ND)
ν_8	2478			100 $\nu_a(ND_2)$
ν_9	2394			100 $\nu_s(ND_2)$
ν_{10}	1544	1565	1565	68 ν(ring) + 17 ν(CX) + 13 δ(CH)
ν_{11}	1471	1483	1481	66 ν(ring) + 34 δ(CH)
ν_{12}	1448	1445		100 $\delta(CH_2)$
ν_{13}	1421		1440	100 $\delta(CH_2)$
ν_{14}	1364	1371	1372	70 ν(ring) + 17 δ(ring) + 13 δ(ND)
ν_{15}	1349	1345	1341	87 $\omega(CH_2)$
ν_{16}	1329			35 $\omega(CH_2)$ + 29 $t(CH_2)$ + 28 ν(ring)
ν_{17}	1314	1317	1319	68 ν(ring) + 11 δ(CH) + 11 $t(CH_2)$
ν_{18}	1267	1260	1261	49 $t(CH_2)$ + 14 $\omega(CH_2)$
ν_{19}	1244			36 $\omega(CH_2)$ + 28 ν(ring) + 15 $t(CH_2)$
ν_{20}	1216	1226	1232	62 δ(CH) + 20 ν(ring)
ν_{21}	1187	1211	1209	88 δ (ND_2) + 10 ν (side chain)
ν_{22}	1173		1174	32 $t(CH_2)$ + 13 ν(ring) + 12 $r(CH_2)$
ν_{23}	1080	1103	1098	47 ν(ring) + 18 δ(CH)
ν_{24}	1051	1069	1073	29 $r(CH_2)$ + 22 ν(side chain) + 12 $t(CH_2)$
ν_{25}	1010	1017	1015	42 ν(side chain) + 13 $r(CH_2)$ + 11 ν(ring)
ν_{26}	984		972	32 ν(ring) + 22 δ(ring) + 10 ν(side chain)
ν_{27}	960	947		38 ν(side chain) + 11 δ(CH)
ν_{28}	914	920	921	72 δ(ring)
ν_{29}	840	852	853	66 γ(CH) + 34 γ(ring)
ν_{30}	835	834	835	51 δ(ND) + 24 γ(CH) + 14 δ(ring)
ν_{31}	828		806	37 ν(side chain) + 18 $r(CH_2)$ + 16 δ(ND) + 13 γ(CH)
ν_{32}	783	779	785	48 γ(CH) + 35 $r(ND_2)$ + 11 γ(CX)
ν_{33}	763		769	38 $\omega(ND_2)$ + 38 γ(CH) + 13 γ(ring) + 10 $r(ND_2)$
ν_{34}	751	763		34 $\omega(ND_2)$ + 24 γ(CH) + 20 $r(CH_2)$ + 13 γ(ring) + 10 $r(ND_2)$
ν_{35}	699	669	675	41 γ(ring) + 23 γ(CX) + 19 r (CH_2)
ν_{36}	638	645	645	36 γ(ring) + 11 $r(CH_2)$
ν_{37}	619	622	626	22 ν(CX) + 16 δ(ring) + 13 γ(ring)
ν_{38}	479		491	62 γ(ND) + 38 γ(ring)
ν_{39}	443			46 δ(side chain) + 28 γ(ring) + 17 γ(ND)
ν_{40}	348		367	52 δ(CX) + 20 τ(side chain) + 14 $r(CH_2)$ + 14 δ(side chain)
ν_{41}	272			50 δ(side chain) + 25 γ(ring) + 13 γ(CX) + 12 δ(CX)
ν_{42}	247			77 $\tau(ND_2)$
ν_{43}	157			34 δ(side chain) + 23 γ(CX) + 21 τ(side chain) + 13 γ(ring)
ν_{44}	95			53 τ(side chain) + 12γ(CX)
ν_{45}	57			100 τ(CX)

[a] Arbitrary numbering. [b] Symbols correspond to the coordinates listed in Table 5. Coordinates with similar characters were added to clarify.

in terms of potential energy distributions allow us to check previous assignments proposed for the infrared and Raman spectra. Assignments proposed for the natural derivative between 1700 and 1200 cm^{-1} were all confirmed. Vibrations ν_{18}, ν_{19}, and ν_{20} were described with significant contributions from both imidazole stretching and methylene bending coordinates. Consequently, the Raman bands at 1322, 1309, and 1267 cm^{-1}, which were measured at 1320, 1308, and 1265 cm^{-1} in the infrared spectrum, have to be better assigned to the two vibrations.

The band at 1160 cm^{-1} was largely assigned to N−H bending vibrations from both imidazole and side chain moieties; however, contributions from the imidazole ring have not been theoretically confirmed. As happened for histamine monocation,[17] the δ(NH) mode is distributed among several normal modes, namely ν_{12}, ν_{14}, ν_{24}, and ν_{25}, Table 7, which makes very difficult to assign it to a single infrared or Raman band. In addition, this fact increases the number of bands that shifts significantly upon N-deuteration, in agreement with the spectral measurements. Thus, the calculated isotopic shifts for the four aforementioned δ(NH) vibrations were, respectively, 12, 68, 32, and 20 cm^{-1}, which can be well correlated to those experimental values, namely 6, 79, 7, and 18 cm^{-1} (all in absolute values). The appreciable deviation for the third vibration, ν_{24}, can be explained at the light of the potential energy distributions for the two isotopomers. As can be checked in Tables 7 and 8, there is not any vibration of the N-deuterated species that can be suitably correlated with the ν_{24} potential energy. In fact, the δ(NH) vibration appears mixed with different coordinates in the natural derivative respect to the N-deuterated one.

Differences between the potential energy distributions of the two histamine isotopomers make also difficult to establish an exact correlation between some of the imidazole stretching vibrations selected in Table 5. The Raman band at 1267 cm^{-1} for natural histamine free-base was calculated at 1251 cm^{-1} and described with significant contributions from imidazole stretching and methylene bending modes. It was initially correlated to the 1261 cm^{-1} band of the N-deuterated derivative, Table 4.

Table 9. B3LYP/6-311G** Scaled Diagonal Force Constants (mdyn/Å or Equivalent Unit) Obtained for Histamine Free Base in an Ellipsoidal Cavity

coord.[a]	symbol	force constant	coord.[a]	symbol	force constant
1	ν (ring)	7.89	24	δ (CH_2)	0.75
2	ν(ring)	5.68	25	δ (side chain)	1.33
3	ν(NH)	6.65	26	ω (CH_2)	0.60
4	ν(ring)	6.75	27	t (CH_2)	0.61
5	ν(ring)	5.34	28	r (CH_2)	0.75
6	ν(CH)	6.41	29	δ (CH_2)	0.79
7	ν(ring)	7.28	30	δ (side chain)	1.45
8	ν(CH)	5.43	31	ω (CH_2)	0.67
9	ν(side chain)	4.52	32	t (CH_2)	0.66
10	ν_s (CH_2)	4.66	33	r (CH_2)	0.93
11	ν_a (CH_2)	4.58	34	δ (NH_2)	0.73
12	ν(side chain)	3.76	35	r (NH_2)	0.76
13	ν_s (CH_2)	4.75	36	ω (NH_2)	0.45
14	ν_a (CH_2)	4.65	37	γ (NH)	0.26
15	ν(side chain)	4.56	38	γ (CH)	0.36
16	ν_s (NH_2)	6.20	39	γ (CH)	0.37
17	ν_a (NH_2)	6.19	40	γ (CX)	0.48
18	δ (ring)	1.80	41	γ (ring)	0.50
19	δ (ring)	1.86	42	γ (ring)	0.56
20	δ (CH)	0.49	43	τ (side chain)	0.07
21	δ (NH)	0.44	44	τ (side chain)	0.16
22	δ (CX)	0.69	45	τ (NH_2)	0.10
23	δ (CH)	0.43			

[a] See Table 5 for coordinate descriptions.

Both wavenumbers were confirmed in the infrared spectra. The calculated wavenumber for deuterated histamine was 1244 cm^{-1}, which establishes an isotopic shift of -7 cm^{-1} for this vibration. However, this assignment necessarily involves the band at 1309 cm^{-1} of the natural derivative has to be also correlated to the aforementioned band at 1261 cm^{-1}. Because no other bands were observed around 1260 cm^{-1} for neutral histamine N-deuterated, we can therefore postulate the existence of an accidental degeneration for the 1261 cm^{-1} band. This conclusion could be considered somewhat surprising because there are not N−H modes involved in these vibrations, at the light of their related potential energy distributions. It is, nevertheless, supported by the comparison between the resulting isotopic shifts for the imidazole stretching vibrations, namely ν_{10}, ν_{11}, ν_{14}, ν_{19}, and ν_{20} from Table 7. The calculated values are -8, -8, -68, -46, and -7 cm^{-1}, respectively; taking into account the precedent discussion, the experimental shifts measured for the involved bands were -5, -7, -79, -48, and -6 cm^{-1}, respectively.

As a general trend, the calculated wavenumbers and normal modes in the region below 1000 cm^{-1} supported the assignments proposed in Table 4. Main disagreements involve to the following bands: (i) the infrared band at 1103 cm^{-1} of the natural derivative was proposed as the second imidazole δ(CH) in-plane vibration. At the light of the normal mode descriptions, the calculated wavenumber more closely described as a δ(CH) vibration in this region was 1071 cm^{-1}, in which a strong mixing with imidazole stretching vibrations exists. Consequently, the second δ(CH) should be better assigned to the 1086 cm^{-1} band of the infrared spectrum. (ii) Bands at 834 and 804 cm^{-1} were assigned to the two imidazole γ(CH) out-of-plane vibrations, while that at 772 cm^{-1} was assigned to a r(CH_2) mode. The theoretical results describe all of them with important γ(CH) characters. Concerning the methylene rocking mode, it exhibits a nonnegligible contribution for the 804 cm^{-1} band. (iii) Amino wagging and C−H out-of-plane vibrations appear extensively mixed. In consequence, the infrared bands at 772 and 763 cm^{-1} have to be similarly assigned to both vibrational modes. (iv) Assignments for the bands measured at 705 and 628 cm^{-1} in the Raman spectrum of the natural derivative could be permuted. However, the two involved normal modes, ν_{35} and ν_{37} (see Table 7) present significant contributions from both imidazole ring and side chain vibrations.

The calculated vibrational spectrum has allowed us also to assign some new bands for neutral histamine in aqueous solution. The Raman bands at 1196 and 604 cm^{-1} have been assigned to a side chain bending vibration and the imidazole γ(NH) mode, respectively, at the light of the potential energy distribution. Similarly, the shoulder measured at 1174 cm^{-1} in the Raman spectrum of N-deuterated histamine can be well correlated to the aforementioned 1196 cm^{-1} band. Deviations respects to the calculated wavenumbers were between 1 and 6 cm^{-1}, in absolute values, which support their assignments.

A relevant fact in order to evaluate the goodness of any force field is the fitting achieved in reproducing the spectra of isotopic derivatives. In the case of neutral histamine, the proposed assignments for the imidazole ND and amino ND_2 bending modes were confirmed by our scaled force field in the most of cases. Thus, the bands at 1209, 835 and 491 cm^{-1} were theoretically described, Table 8, as 88%-δ(ND_2), 51%-δ(ND) and 62%-γ(ND), respectively. Other vibrations of the deuterated amino group, as r(ND_2) and ω(ND_2), are relevant contributions in several normal modes, which do not allows for an unambiguous assignment to a single band.

The scaled diagonal force constants are listed in Table 9. As happened for histamine monocation in solution,[17] the force constants for the imidazole stretching coordinates are consistent with a localized bond description where the double bonds would be at N1−C2 and C4−C5 positions. The obtained values are one-to-one near to those reported for the monocation, which indicates a similar electronic distribution for the imidazole rings. We have to take into account, nevertheless, that this moiety has 1/3 of the monocation ionic charge, whereas it is almost neutral in the free base. In our opinion, this difference could be compensated by the structural specificities of the relevant conformations, trans for the monocation and gauche for neutral histamine. Thus, the gauche conformation allows for interaction between the amino group and the imidazole ring, which could has some influence in the force constants. Concerning the rest of stretching force constants, there are not significant deviations respects to those reported for histamine monocation.

Conclusions

The structures of four relevant tautomers of histamine free-base in solution have been optimized by quantum-mechanical methods, at the B3LYP/6-311G** level, and a continuum solvent model. Calculated free energies were in the order t1 > t3 > g1 > g3, which establishes the g3 conformer as the most stable one. Quadratic force fields were computed, under the same theoretical scheme, for the four aforementioned tautomers. After a general assignment of the infrared and Raman spectra of neutral histamine in solution of H_2O and D_2O, wavenumbers for the imidazole ring stretching and bending vibrations were compared to the calculated ones, previously scaled by a generic factor of 0.97 applied to the force constants. The calculated-experimental differences clearly indicate that histamine free-

base in aqueous solution is in the N^{τ} form. Quadratic mean deviations were 10−15 cm^{-1} higher for the N^{π} form respect to the N^{τ} ones. In addition, they were 6−7 cm^{-1} higher for the t3 than for the g3 conformer, which supports the free-energy calculations. The calculated infrared intensities were also in agreement with this conclusion. The predicted spectral pattern for the N^{τ} structures fitted better to the experimental infrared spectra than the N^{π} structures, the g3 conformer giving a better result than the t3 one. The g3 conformer was selected for a further vibrational dynamics calculation, in which a low-scaling procedure (only three generic scaling factors) was first performed. The obtained normal modes allowed us to check our prior assignments, mainly based on the isotopic shifts upon deuteration.

Thus, both experimental and theoretical evidences seem to agree in the fact that g3 is the most stable conformer of histamine free-base in aqueous solution. This is in contrast to histamine monocation in solution, for which t3 has been suggested as the most stable form. In this last molecule, the presence of a positively charged side chain leads to adopt an extended conformation, which allows it for a deeper interaction with the solvent molecules. The predicted structure of neutral histamine in solution also differs from that reported in gas phase, which was g1. This conformation allows for an intramolecular interaction between the amino group and the imidazole ring, although it is not suitable for interaction with surrounding molecules.

Acknowledgment. The Spanish Ministry of Science and Technology (grant BQU2000-1425) has supported this work. Authors thanks to M. Roca and S. Martí for assisting them with the QM/MM MD simulation.

Supporting Information Available: Full scalled B3LYP/6−311G** force field matrix for the Cartesian coordinates for the minimum (g3)−H_2O. This material is available free of charge via the Internet at http://pubs.acs.org.

JA027103X